Reduction of Proximity Effects on UHF Passive RFID Systems by Using Tags With Polarization Diversity

Qi Zhang, *Student Member, IEEE*, Michael. J. Crisp, *Member, IEEE*,
Richard V. Penty, *Senior Member, IEEE*, and Ian H. White, *Fellow, IEEE*

Abstract—A new technique that enables passive ultra high frequency (UHF) radio frequency identification (RFID) tags to be read when they are placed in close proximity in an array is presented. This paper demonstrates that, in a linear tag array with a tag separation of 1 cm, the interaction between the backscattered waves and incident wave causes a significant degradation in tag sensitivity. It is found that the use of tags that have polarization diversity can improve the read performance when they are placed in close proximity to one another compared with conventional linear tags. Two ways of achieving polarization diversity are studied in this paper, namely: 1) using a circularly polarized tag and 2) using a cross-polarized tag pair. Both methods show an improvement in close proximity read performance and it is experimentally demonstrated that by using cross-polarized tag pairs in an array, one achieves on average a 2.6-dB increase in read power margin for a 57-tag array with 1 cm separation compared with using conventional linearly polarized tags.

Index Terms—Circularly polarized tag, close proximity, passive ultra high frequency (UHF), polarization diversity, radio frequency identification (RFID), tag pairs.

I. INTRODUCTION

IN RECENT years, radio frequency identification (RFID) technology has been used in a wide range of mainstream applications [1]–[3] and passive ultra high frequency (UHF) RFID tags are increasingly replacing current barcode systems due to their longer range, high data capacity, faster read speed, and programmability [4]. Passive UHF systems operate on the principle of backscatter communications with the tag antenna gathering energy from the electromagnetic wave transmitted by the reader, and then using the energy to power a microchip. This then changes the load on the antenna to achieve backscatter modulation and communication back to the reader. Previously, it has been suggested that RFID tags need to be separated from each other by around 10 cm in order to be reliably detected without significantly increasing the required radio frequency (RF) power [5]. This is clearly not practical for many applications such as item level tagging of small tightly

packed objects. Therefore, a simple tag configuration to reduce proximity effects is investigated.

The major causes of tag sensitivity degradation in arrays are analyzed in [6]–[9]. It has been shown that different effects such as tag detuning, tag shadowing, and re-radiation cancelation operate over different length scales of separation. Tag detuning is caused by power loss due to a mismatch between the tag antenna and IC, which originates from the impedance change of the tag antenna when one tag approaches another. It is shown that detuning has a significant effect when tags are placed very close to one another and has less influence when tags are placed at separations greater than 1 cm [6]–[8]. Tanaka *et al.* [7] have proposed a solution to extend the tag read range by changing the RFID integrated circuit chip impedance to compensate for the impedance mismatch caused by the antenna. Research has also been carried out on designing tag antennas, which are able to operate close to a metallic surface [10]–[12].

For tag arrays, it has been demonstrated that tag shadowing and re-radiation cancelation between the backscattered waves from other tags in the array and the incident wave have a significant effect on the read performance of tags [3], [13], [14]. Weigand *et al.* [15] suggested that multiple planes of RFID tag antennas produce interference effects and the array geometry may have an important effect on the ability to read tags reliably. In [6], it is shown through both simulation and experiment that the backscattered waves and the incident wave can combine in a manner that forms an interference pattern similar to that observed in other systems of multiple reflectors such as Bragg gratings. For many commercial passive UHF RFID applications, a circularly polarized reader antenna is employed to achieve orientation diversity, and the RFID tags are designed with a dipole or microstrip-type antennas with linear polarization [16]. In this case under free space transmission conditions, only half of the potential power transmitted from the reader can be received by the tag antenna as the polarization efficiency is -3 dB. However, if the tag antenna has polarization diversity and is not only able to receive signal in one single linear polarization, polarization matching between the reader and tag antenna can be realized, which can lead to maximum power transfer [17]. More importantly, the problem of re-radiation cancelation can be greatly reduced if tags with polarization diversity are used owing to the reduced interaction of the reflected waves.

For the first time, a new technique using tags with polarization diversity instead of normal linear polarization to reduce the problem of re-radiation cancelation is presented. Two methods of achieving polarization diversity are studied. One method is to use a circularly polarized tag, which is able to produce a circularly polarized backscattered wave. The other method is to use a cross-polarized tag pair, which is fabricated by placing two linearly polarized tags close together with orthogonal polarization directions. Both the methods are demonstrated through experiment or simulation showing that the tag read performance is greatly improved when such tags are placed close to each other in an array compared to the conventional case that uses linearly polarized passive tags.

II. Tag Re-Radiation Cancelation

Tag re-radiation cancelation is caused by the re-radiated waves from the tag and the incident wave from the reader combining in a manner that leads to interference. In certain locations, the interference is destructive and prevents tag detection. It is difficult to observe this directly through experiment as other multipath effects in real environments have a significant effect on the power available at each tag in the array, making it difficult to decouple multipath effects from proximity effects.

In our work, FEKO, an electromagnetic simulation software tool based on the method of moments (MoM) technique [18], is used to simulate a tag array to study the effect in more detail. To act as a benchmark, a simple wire model of a passive UHF RFID tag is created approximating the tag to a folded dipole antenna with a T-matching network, as shown in Fig. 1. The dimensions of the tag model are also indicated in Fig. 1. Simplifying the tag structure reduces the complexity and processing time of the simulation. The microchip of the tag is modeled as a complex load impedance, which is set to be the conjugate match of the tag antenna to ensure optimal power transfer into the chip. The folded dipole provides great freedom for impedance adjustment especially for the imaginary part that helps in the impedance matching of practical tag chips. The tag is optimized to work at an operating frequency of 865.1 MHz.

An array of 57 linear tags with a tag separation distance of 1 cm is simulated. It has a tag array length of 56 cm, which is greater than the wavelength at transmission frequency used in free space. The 1-cm tag separation is chosen as it represents a typical tag separation needed in, e.g., retail applications being about the same size as the width of books, CDs, or coat hangers, etc. The incident wave is linearly polarized with a frequency of 865.1 MHz and has a uniform field strength of 1 V/m. The test is carried out with the incident wave fronts orthogonal to the long axis of the array with tag ID 1 closest to the excitation source as shown in Fig. 2. The simulated power received by the load (which represents the IC) for each tag is recorded and the change in power received at each tag IC normalized to single tag case is plotted against its position in the array in red as shown in Fig. 3.

It can be seen in Fig. 3 that for linearly polarized tag array (shown as red curve), the power captured by the IC does not
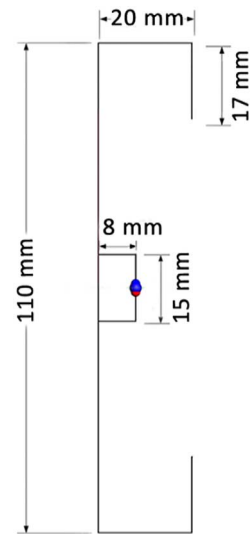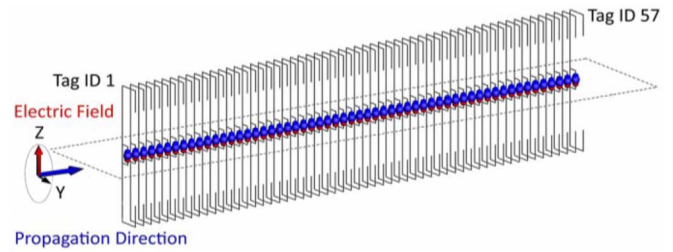

Fig. 1. Model of a single tag.

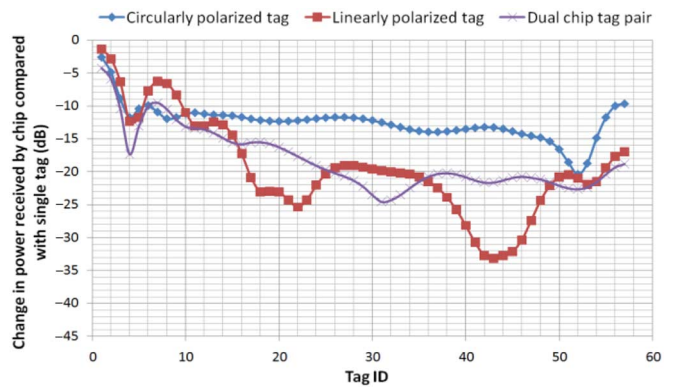Fig. 2. Model of a linear tag array.

Fig. 3. FEKO simulated normalized power into chip (dB) against tag ID.

simply follow a decreasing trend (as it would if tag shadowing was dominant). The tag closest to the radiation source (tag ID 1) indeed has the highest captured energy compared with other tags in the array and the curve generally follows a decreasing trend until about two-thirds through the array. The shape of the plot, however, shows a cyclical behavior with noticeable nulls around tag ID 20 and tag ID 43 and a slowly increasing trend at the end of the array. A 17-dB more power is received by the IC in the furthest tag (tag ID 57) away from the excitation source compared with the tag that captures the least amount of energy in the array (tag ID 43). This indicates that shadowing is not the only effect that plays an important role.
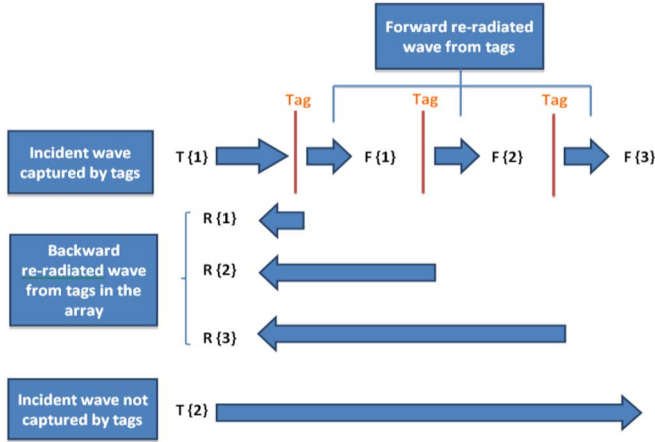
Fig. 4. 2-D MATLAB model.

Fig. 5. MATLAB simulated normalized power into chip (dB) against tag ID.

FEKO software is used to perform a full EM simulation taking into account of all the factors including energy coupling and detuning. Therefore, in order to separate out and determine the impact of re-radiation cancelation and confirm that the effects seen in Fig. 3 are also predominantly caused by the interaction between incident wave and backscattered waves from the tags, a simple two-dimensional (2-D) MATLAB model is created for the system.

The model considers a similar situation as above with an incident wave coming from one end of the array with tag ID 1 closest to the excitation source. Fig. 4 explains the operation of this model. The model makes the simplifying assumptions that the backward re-radiation wave does not cause secondary radiation from the previous tags in the array and the tag has a negligible thickness. When the incident wave meets a tag in the array, a proportion of its energy is captured by the tag indicated as T{1} and the rest passes through freely indicated as T{2}. Some of the energy captured is absorbed by the tag, while some is reflected creating forward and backward re-radiation waves with a phase shift indicated as F waves and R waves in Fig. 4. The energy absorbed by the next tag is the complex sum of the forward re-radiated wave from the previous tag in the array, the backward re-radiated waves and the incident wave. An iterative process is used until a steady state solution is found taking the backward re-radiated waves to be zero as an initial condition. For example, to calculate the forward and backward re-radiated waves at the ith tag in an array of N tags in total

$$\text{F}\{i\} = Ae^{i\emptyset}\,(\text{F}\{i-1\} - \text{R}'\{i\} - \text{R}'\{i+1\}$$
$$\qquad - \cdots - \text{R}'\{N\}) \qquad\qquad (1)$$
$$\text{R}\{i\} = Ae^{i\emptyset+\pi}\,(\text{F}\{i-1\} - \text{R}'\{i\} - \text{R}'\{i+1\}$$
$$\qquad - \cdots - \text{R}'\{N\}) \qquad\qquad (2)$$

where A is the amplitude change and $\emptyset$ represents the phase change. The minus sign indicates that the waves are traveling in the opposite direction to the incident wave. R' is the calculated backward re-radiated wave from the previous iteration.

The incident wave is linearly polarized and the polarization is in the same plane as to the tags in the array, with a frequency of 865.1 MHz and a field strength of 1 V/m. The tag array consists
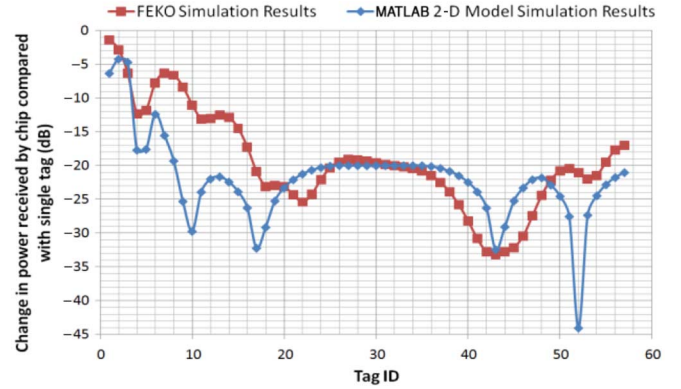
of 57 uniformly spaced tags at 1 cm separation to match the parameters of the FEKO model.

Fig. 5 shows the simulated power received at each tag in the MATLAB model normalized to the single tag case against tag position within the array in blue. The simulation results from FEKO in Fig. 3 are also plotted in the same figure for comparison. It is seen that the simulation results from the simple 2-D MATLAB model qualitatively agree with the results seen in FEKO EM simulation software in Fig. 3. Both results show an interference pattern with deep nulls around tag ID 20 and tag ID 43. Very close agreement is not expected as the MATLAB model only considers the interference between backward re-radiated waves and incident wave, whereas the FEKO model performs a full electromagnetic analysis, which takes into account all other factors such as inductive coupling between neighboring tags. However, the similarity of the null positions between the simulation results from these two models shows that the dominant effect must be included in the MATLAB model, which is the re-radiation cancelation between the incident wave and the backscattered waves from the tags.

III. CIRCULARLY POLARIZED TAG ARRAY

A. Circularly Polarized Tag

It is a common practice to use circularly polarized interrogator waves to reduce the polarization dependence of detection at a RFID tag of unknown orientation [16]. This is because the use of circularly polarized waves and linear polarized tags prevents a complete mismatch occurring between the tag polarization and the interrogation signal polarization for certain tag orientations. A vertically polarized tag is able to detect the vertical component of the circularly polarized transmission wave from the interrogation antenna and produces a vertically polarized backscattered wave and similarly, a horizontally polarized tag is only able to respond to the horizontal component of the circularly polarized transmission wave.

It is found in Section II that re-radiation cancelation is one of the effects that limits tag read performance when tags are placed with small separations in an array. The linear backscattered waves from the tags interact with each other, as well as the incoming incident wave, and produce destructive interference at some position along the array. For a linear polarization,
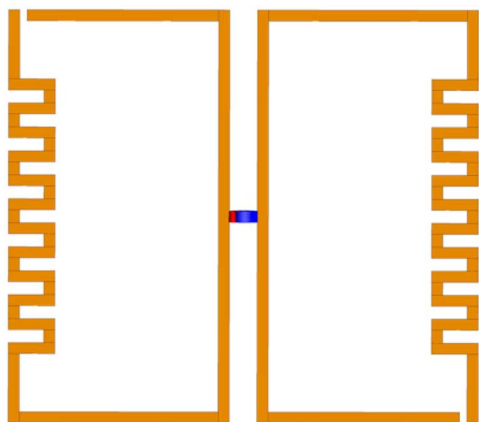
Fig. 6. Model of a circularly polarized tag.

Fig. 7. Axial ratio of the circularly polarized tag model.

Fig. 8. Model of a circularly polarized tag array.

the forward traveling wave affects the amplitude seen by tags further down in the array. The backscattered waves interfere with each other and the incident wave that produces an inference pattern. However, in the case of circularly polarized waves reflecting from circularly polarized tags, the reflected and incoming waves have opposite handedness, thus reducing the interference. Using circularly polarized tags to label one object, it is possible to detect a signal in either linear polarization. Therefore, even if the signal in one particular polarization is significantly degraded, the forward link signal can still be successfully detected as the less degraded signal in the other polarization can still be captured by the circularly polarized tag.

B. Circularly Polarized Tag Array Model

A circularly polarized tag model is simulated in FEKO software as shown in Fig. 6. The tag model follows that of Bjorninen *et al.* [19]. A complex impedance is used in the model to represent the RFID tag chip and its value is chosen to be the complex conjugate of antenna impedance to maximize power transfer. To demonstrate that this tag indeed produces a circularly polarized backscattered wave, the tag pair model shown in Fig. 6 is excited with a linearly polarized wave with field strength of 1 V/m at 865.1 MHz. The polarization angle of the linear incident wave is varied from 0° to 180° and the simulated power received by the ICs for each case is recorded. The axial ratio, which is defined as the ratio of the major axis to the minor axis of the polarization ellipse, is used to measure the degree of circular polarization. For the tag model, based on the simulation results, the axial ratio is calculated to be 1.6 at our test frequency. The results of the simulation of axial ratio against frequency for the circularly polarized tag model are illustrated in Fig. 7. The same simulation procedure is also applied for the linear tag model shown in Fig. 1 giving an axial ratio of 70.4 at an operating frequency of 865.1 MHz. Usually, the axial ratio needs to be less than 3 dB for an antenna to be considered as circularly polarized [20], [21]. This demonstrates that the designed tag model exhibits good circular polarization

A tag array consisting of 57 such tags with a tag-to-tag separation of 1 cm is simulated as shown in Fig. 8. The excitation
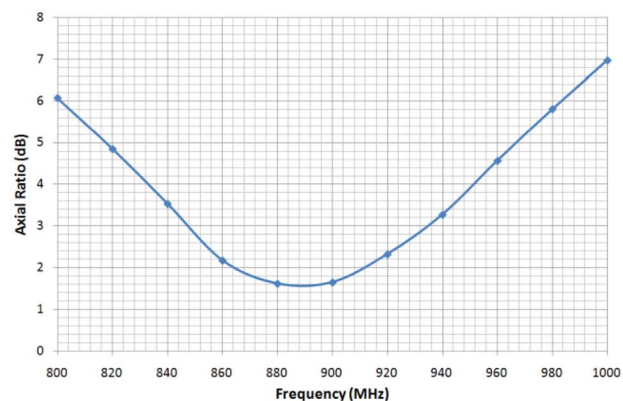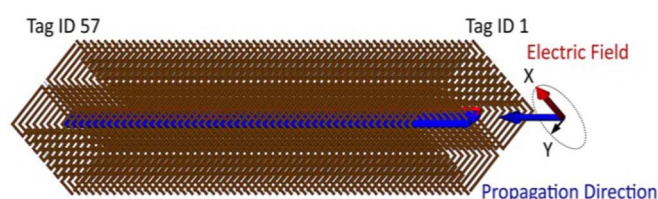
source is positioned at one end of the array with tag ID 1 closest to the excitation source. The array is excited with a right-handed circularly polarized wave (the incident wave is matched to the handedness of polarization to the tag) with field strength of 1 V/m at 865.1 MHz. The power received by each tag IC within the array is recorded. This is then normalized with respect to the power received by the tag IC when only a single tag of the same design is present under the same incident wave. The change in power received by tag IC compared to the single tag case is plotted against tag ID in blue in Fig. 3.

From the normalized power received by the tag ICs in the linearly polarized tag array plotted in red in the same figure, it is seen that for both linearly polarized and circularly polarized tag arrays, the power received by the tag IC reduces when tags are placed in an array compared with single tag case. Both of these arrays show the tag shadowing with tags close to the excitation source tending to capture more energy than tags further away. One noticeable difference between these two curves, however, is that the decreasing gradient of normalized received power for the linearly polarized tag array is much larger than that for the circularly polarized tag array. More importantly, the cyclical behavior with deep nulls seen in the linearly polarized array does not appear in the circularly polarized array. It is observed that the normalized received power for the circularly polarized tag array is much larger than the linearly polarized tag array, which implies much smaller tag performance degradation when the tag is placed in close proximity in an array compared with the single tag scenario. Before tag ID 14, tags in both arrays have similar performance. After that, a deep null forms around tag ID 20 in the linear tag array. However, the normalized power at tags in the circular array remains at roughly the same value. As discussed in Section III-A, the reason for the absence of deep nulls being observed in the circular array is that
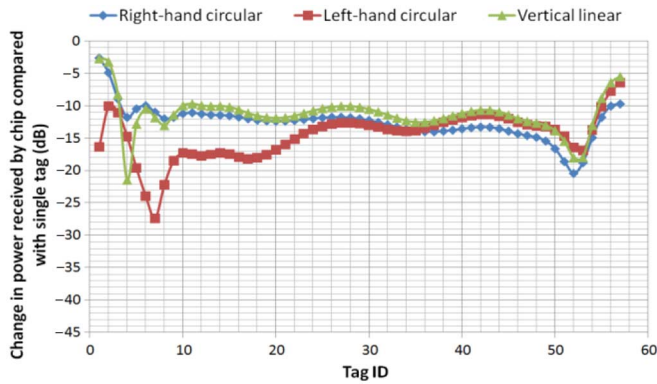
Fig. 9. Normalized power into chip (dB) against tag ID in a circularly polarized tag array under different interrogating waves.

Fig. 10. Model of a cross-polarized tag pair.

Fig. 11. Model of a tag pair array.

a circularly polarized tag produces a circularly backscattered wave with opposite handedness to the incident wave. When these waves interfere, an elliptically polarized wave is formed. Even if there is complete cancelation in one polarization, the circularly polarized tag is still able to detect the incoming signal in the orthogonal polarization. However, a linearly polarized tag is only able to detect and backscatter the signal in the same polarization as the tag itself. When the signal in this particular polarization plane degrades due to re-radiation cancelation, the tag performance at these positions degrades and nulls in normalized received power are seen. Comparing the worst case in both tag arrays, at tag ID 43 where the largest reduction in received power for linear tag array occurs, the reduction in received power for circularly polarized tag is 22 dB better. Similarly, at tag ID 53, where reduction is most significant for circularly polarized array, the reduction is still 1 dB better than the tag at the same position in linear array. Therefore, a circularly polarized tag array has demonstrated a much better performance than conventional linearly polarized tag arrays when tags are placed in close proximity.

Fig. 9 shows the simulated results of the change in received power at each tag IC compared to a single tag in isolation under interrogating waves with different polarizations. It is observed that the circularly polarized tag array is sensitive to the handedness of the incident wave. When an incident wave with orthogonal circular polarization to the tag is seen by the array (left-handed circularly polarized wave in this case), very little energy is captured by the tag IC. However, if a matched incident wave is seen by the array, a much better performance is achieved (right-handed circularly polarized wave in this case). The simulated results under linear excitation have a similar performance to matched circular excitation.

IV. CROSS-POLARIZED TAG PAIR ARRAY

A. Cross-Polarized Tag Pair Array Model

In this work, we have also sought to study the performance of a "tag pair" consisting of two cross-polarized linear tags placed very close to each other (as shown in Fig. 10). The tag pair is of interest as it allows the two polarization components to be detected separately. An array of tag pairs is again simulated
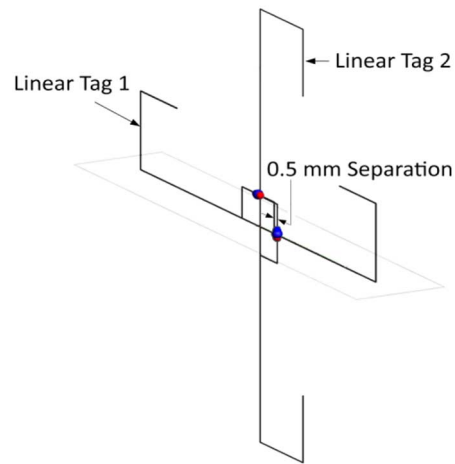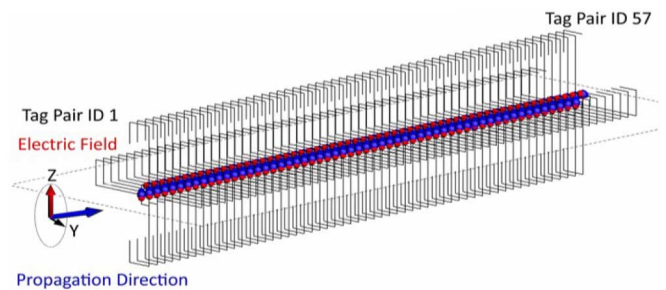
in FEKO software. The same linear RFID tag line model in Section II is used to create the tag pair. Each tag pair consists of two linearly polarized RFID tags, which are placed close to each other at 0.5-mm spacing with orthogonal polarization directions.

The power received by the tag pair is defined as the maximum of the power received by each tag IC of the vertical and horizontal tags within each pair. A simple test is carried out to look at the polarization of a single tag pair. A linear polarized wave with field strength of 1 V/m at 865.1 MHz is used to excite the tag pair and its polarization angle is varied from 0° to 180°. For each case, the power received by the tag pair is recorded. It is calculated that the ratio of the power received in major axis and minor axis is 4.5 dB, which is worse than the circularly polarized tag model shown in in Section III. However, it is worth noting that since the pair is polarization diverse rather than truly circularly polarized, it will not be possible to mismatch the incident wave polarization.

A tag pair array consists of 57 tag pairs with a separation distance of 1 cm in between adjacent pairs is simulated as shown in Fig. 11. The incident wave comes from one end of the array with tag pair ID 1 closest to the excitation source. A right-handed circularly polarized wave with field strength of 1 V/m at 865.1 MHz is used as the incident wave.

In Fig. 3, the normalized power received by the cross-polarized tag pair (the maximum between the horizontal and vertical tag captured power) with respect to a single tag pair is plotted in purple, and the simulated results for a linear tag
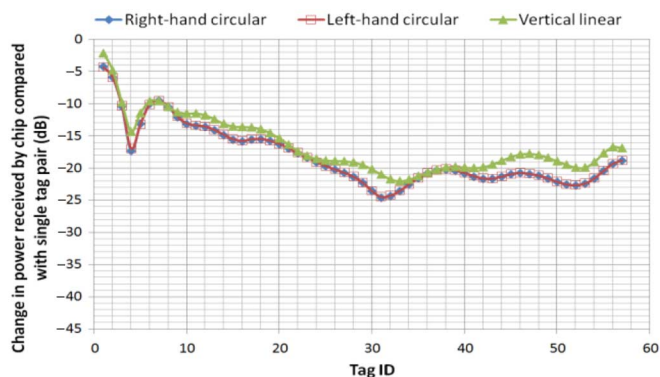
Fig. 12. Normalized power into chip (dB) against tag ID in a tag pair array under different interrogating waves.

Fig. 13. Experiment arrangement.

array and a circularly polarized tag array are also plotted for reference in blue and red, respectively. It is observed that the cross-polarized tag pair array has much better performance than the linear tag array as the reduction in the power received at the worst tag in the tag pair array is 10 dB higher than in the linear tag array. The main improvement occurs in two-thirds of the array furthest from the excitation source. For the first 14 tags, both cross-polarized tag pairs and linear tags have similar performance. Both the curves have a sharp reduction in the power received at the IC around tag ID 4. After tag ID 14, the normalized power received at tag in the linear tag array starts to decrease significantly and it has a cyclical behavior with deep nulls around tag ID 20 and tag ID 44, whereas the power received at the tags in the cross-polarized tag pair array smoothly decreases with much smaller decreasing gradient between tag ID 10 and tag ID 20, then the normalized power received at tag ICs reaches a steady value of around -22dB. At tag ID 20 and tag ID 43, where the deep nulls in the tag received power in the linear array are located, the cross-polarized tag pair helps to improve the normalized tag received power by 8 dB and 11 dB, respectively. It is seen from the simulation results that the cross-polarized tag pair array improves the tag read power margin compared to the conventional linear tag array, but is not as good as the circularly polarized tag when excited with matched polarization. One possible reason for this is that the tag pair used here has a worse "axial ratio" than the circularly polarized tag used in Section III. This implies the tag pair in this model does not produce as good diversity in the horizontal and vertical polarization planes as the circularly polarized tag model.

Fig. 12 shows the simulated change in power received at tag ICs under interrogating waves with different polarizations. It is seen that, unlike the circularly polarized tag array, in this case, the tag array is not sensitive to the handedness of the circular polarization of the incident wave. The simulated results under right-handed circularly polarized wave (in blue) and left-handed circularly polarized wave (in red) completely overlap. The results under linear excitation tend to have a similar performance to those under circular excitation with some minor improvement of 2–3 dB at some positions along the array.
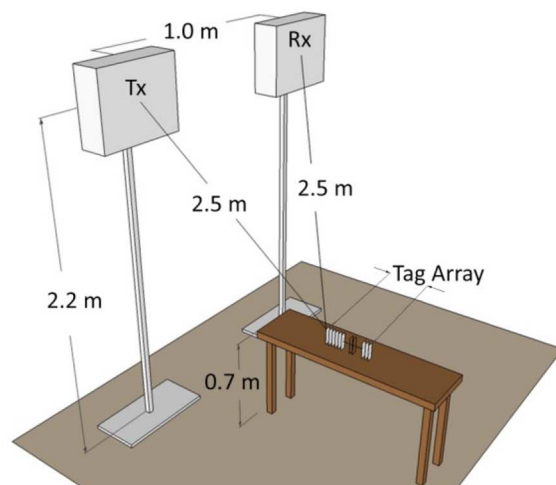
B. Experiment Results

An experiment is carried out to test the performance of the cross-polarized tag pair in an array in a real laboratory environment and the result is then compared to that of a conventional linear tag array. The passive circularly polarized UHF RFID tags are not tested here because they are currently not available commercially. The experiment arrangement is shown in Fig. 13. A bistatic antenna configuration with a separation of 1 m between the transmitting and receiving antennas (Tx and Rx) is used, so that sufficient isolation is afforded for the experiments to ensure a high reader sensitivity and therefore a downlink limited link. The isolation between reader antennas is determined by connecting both antennas to a VNA and then measuring the transmission coefficient S_{12} between two ports while varying the horizontal separation between the antennas. The isolation between the antennas at 1 m is 50 dB and it is seen that no further increase in reader's sensitivity occurs when higher antenna isolation is applied. Reader antennas are placed 2.2 m above the ground to represent a practical environment where reader antennas are positioned high over the ground to provide a wider coverage area. The high mounting of antennas in a practical situation also avoids the antenna becoming physical obstacles. The antennas are left-handed circularly polarized antennas with 6 dBi gain and 70° beam width operating in the European Telecommunications Standard Institute (ETSI) frequency band of 865–867 MHz. The cross-polarized tag pairs used in this experiment are fabricated by placing two linearly polarized tags closed together with a separation of 0.5 mm with orthogonal polarization directions, which is the same method as used in the simulation model shown in Fig. 10. The tags used in the experiment are UMP DogBone™ inlays using Impinj Monza 4 ICs, which are effectively a short wide-loaded dipole with a T-matching network as shown in Fig. 14.

The reader is programmed to vary the transmission power from 36 to 12 dBm EIRP at fixed transmission frequency of 865.1 MHz. The minimum transmission power needed to detect each tag pair successfully within the array is recorded. For each cross-polarized tag pair, both minimum transmission powers for vertical and horizontal tags are recorded and the smaller value

Fig. 14. Impinj Monza 4 tag.

Fig. 15. Normalized tag read power margin (dB) against its position within tag pair array.

is treated as the minimum transmission power needed to detect the cross-polarized tag pair. The read power margin for each tag pair is defined as the ratio in dB of the maximum allowed transmission power and the minimum power needed for successful detection. The maximum transmission power from the reader is limited by regulations, usually set to be 36 dBm EIRP [22]. The read power margin of each tag pair is then subtracted from that measured from a single tag without the presence of other tags. In this way, we substantially exclude multipath effects and only measure the changes in read power margin of tags in the array with respect to single tag case. Both experiment and simulation results focus on normalized value (power received at tag IC or tag read power margin), and only considers the change in these values when tags are placed in close proximity compared to that measured in the single tag. The folded dipole line model in FEKO (shown in Fig. 1) aims to represent a general UHF passive tag instead of a specific tag design. Therefore, the antenna properties such as antenna gain and radiation pattern do not need to be exactly the same in order to be able to compare the simulation and experiment results.

The same experimental procedure is repeated for the cross-polarized tag pair array and linear tag array. Both the arrays have a tag-to-tag separation distance of 1 cm. The tag array is placed at a distance of 2.5 m from the antennas. The measurements are taken with the tag array positioned such that the long axis of the array is orthogonal to the interrogator wave fronts with tag ID 1 closest to the antennas. Other tag array orientations with respect to the excitation source are considered in [6] such as with the array parallel to the interrogator wave fronts. It is found in [6] that the tag array configuration used here is the best tag array orientation, i.e., the one which has the smallest worst case tag sensitivity penalty. Fig. 15 presents the normalized read power margin for each tag or tag pair with respect to the single tag case against tag ID within the array. The normalized power margin for tag ID 47 and 50 is not shown in Fig. 15, which indicates that both tags cannot be detected by the reader even at the maximum transmission power.

It is observed that, in general, the tags in the linearly polarized tag array have much larger reduction in their read power margin than tags in the cross-polarized tag pair array. This result agrees qualitatively with the simulation result in Fig. 3. It is seen clearly that for the linearly polarized tag array, there exist certain sections of the tag array where the tag performance becomes worse than others, e.g., around tag ID 22 and tag ID 40. This is very similar to the cyclical behavior with nulls shown in the simulated results for the linear array shown in Fig. 3. The experimental result for the cross-polarized tag pair array features a slowly decreasing trend, which is also similar to the simulation results. However, exact agreement is not
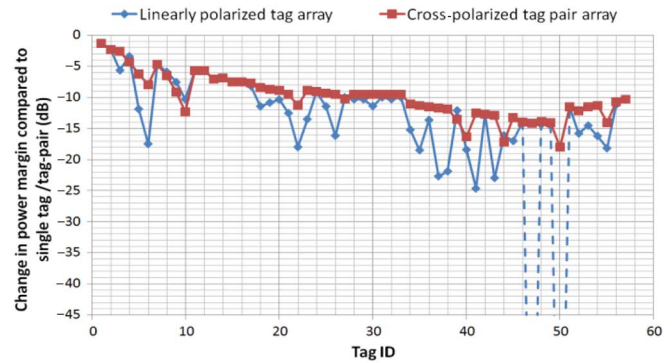
expected because the computer simulation does not take into account of the factors such as the manufacturing variations in tags. The difference in the normalized tag read power margin seen in the experiment can be as large as 10 dB and the average improvement of the normalized read power margin is calculated to be 2.6 dB (excluding the situation when some tags are not detected in linear tag array, but are detected in cross-polarized tag pair array).

V. CONCLUSION

We have demonstrated that, using both EM simulation software and a theoretical model that for a tag array with separation of 1 cm, the interference between backscattered waves from tags and the incident wave from the reader causes significant degradation in tag sensitivity. We study the use of tags with polarization diversity in close proximity in a tag array to improve the read performance. Two methods to reduce proximity effects and also polarization dependence have been studied, namely using circularly polarized tags and cross-polarized tag pairs. Both the methods are demonstrated through software simulation or experiment showing that better tag read performance for arrays with close proximity is achieved compared to conventional linearly polarized tags. Our results show that circularly polarized tags tend to have better performance than cross-polarized tag pairs owing to their better axial ratio. However, they are limited in that the incident wave needs to be matched to the handedness of the tag. Cross-polarized tag pairs are not sensitive to the handedness of the incident wave. It is shown through experiment in a real laboratory environment that using the cross-polarized tag pairs improves the tag read performance by 2.6 dB on average (excluding the situation when some tags are not detected in the linear tag array, but are able to be detected in the array of cross-polarized tag pairs) and the most significant improvement can be as large as 10 dB. Based on simulation results from FEKO, circularly polarized tags with a better axial ratio may lead to further improvements.

REFERENCES

[1] N. Li, W. Ni, H. Cheng, and J. Tan, "A systememematic RFID application platform with intrgration capability for tour and exhibition," in *Proc. IEEE Int. Conf. RFID Technol. Appl. (RFID-TA)*, 2011, pp. 37–44.

[2] D. Yue, X. Wu, and J. Bai, "RFID application framework for pharmaceutical supply chain," in *Proc. IEEE Int. Conf. Serv. Oper. Logist. Inf. (SOLI)*, 2008, vol. 1, pp. 1125–1130.

[3] D. Lee, S. Kim, H. Kim, and N. Park, "Mobile platform for networked RFID applications," in *Proc. 7th Int. Conf. Inf. Technol.*, 2010, pp. 625–630.

[4] K. Finkenzeller, *RFID Handbook: Fundamentals and Applications in Contactless Smart Cards and Identification*, 2nd ed. Hoboken, NJ, USA: Wiley, 2003, pp. 29–180, 229–328.

[5] (2014). *United States Department of Defense Suppliers' Passive RFID Information Guide*, Version 15.0, p. 20 [Online]. Available: http://www.acq.osd.mil/log/sci/ait/DoD_Suppliers_Passive_RFID_Info_Guide_v15update.pdf.

[6] Q. Zhang, M. Crisp, I. H. White, and R. V. Penty, "Power margin reduction in linear passive UHF RFID tag arrays," in *Proc. IEEE Int. Conf. RFID-Technol. Appl. (RFID-TA)*, 2014, pp. 312–317.

[7] Y. Tanaka, Y. Umeda, O. Takyu, M. Nakayama, and K. Kodama, "Change of read range for UHF passive RFID tags in close proximity," in *Proc. IEEE Int. Conf. RFID*, 2009, pp. 338–345.

[8] H. Yojima *et al.*, "Analysis of read range for UHF passive RFID tags in close proximity with dynamic impedance measurement of tag ICs," in *Proc. IEEE Radio Wireless Symp. (RWS)*, 2011, pp. 110–113.

[9] D. Dobkin, *The RF in RFID Passive UHF RFID in Practice*. Amsterdam, The Netherlands: Elsevier, 2008, pp. 345–346.

[10] D. M. Dobkin and S. M. Weigand, "Environmental effects on RFID tag antennas," in *Proc. IEEE MTT-S Int. Microw. Symp. Dig.*, 2005, pp. 135–138.

[11] M. S. Alkhambashi *et al.*, "A novel RFID tag antenna mountable on metallic objects," in *Proc. IEEE Int. Conf. Microw. Millimeter Wave Technol. (ICMMT)*, 2008, vol. 4, pp. 1822–1824.

[12] Tashi, M. S. Hasan, and H. Yu, "Design and simulation of UHF RFID tag antennas and performance evaluation in presence of a metallic surface," in *Proc 5th Int. Conf. Softw. Knowl. Inf. Ind. Manage. Appl. (SKIMA)*, 2011, pp. 1–5.

[13] H.-D. Chen, S.-H. Kuo, C.-Y.-D. Sim, and C.-H. Tsai, "Coupling feed circularly polarized RFID tag antenna mountable on metallic surface," *IEEE Trans. Antennas Propag.*, vol. 60, no. 5, pp. 2166–2174, May 2012.

[14] M. Buzzi, M. Conti, C. Senette, and D. Vannozzi, "Measuring UHF RFID tag reading for document location," in *Proc. IEEE Int. Conf. RFID-Technol. Appl. (RFID-TA)*, 2011, pp. 115–122.

[15] S. M. Weigand and D. M. Dobkin, "Multiple RFID tag plane array effects," in *Proc. IEEE Antennas Propag. Soc. Int. Symp.*, 2006, pp. 1027–1030.

[16] B. Yu, S. J. Kim, B. Jung, F. J. Harackiewicz, and B. Lee, "RFID tag antenna using two-shorted microstrip patches mountable on metallic objects," *Microw. Opt. Tech. Lett.*, vol. 49, no. 2, pp. 414–416, 2007.

[17] Y.-M. Tseng, S.-H. Kuo, H.-D. Chen, and C.-Y.-D. Sim, "Circularly polarized circular microstrip RFID tag antenna," in *Proc. Microw. Conf.*, 2012, pp. 1142–1144.

[18] FEKO Software [Online]. Available: https://www.feko.info

[19] T. Bjorninen, L. Ukkonen, L. Sydanheimo, and A. Z. Elsherbeni, "Circularly polarized tag antenna for UHF RFID," in *Proc. 26th Annu. Rev. Prog. Appl. Comput. Electromagn.*, 2010, pp. 372–375.

[20] M. Sumi, K. Hirasawa, and S. Shi, "Two rectangular loops fed in series for broadband circular polarization and impedance matching," *IEEE Trans. Antennas Propag.*, vol. 52, no. 2, pp. 551–554, Feb. 2004.

[21] S. Gao, Q. Luo, and F. Zhu, *Circularly Polarized Antennas*. Hoboken, NJ, USA: Wiley, 2014, pp. 5–6.

[22] D. D. Deavours. (2005). *UHF EPC Tag Performance Evlaution* [Online]. Available: http://www.rfidjournal.net/ Alliance_Lab_Report_intro.pdf

Michael J. Crisp (S'07–M'10) received the M.Eng. and M.A. degrees in electronics from the University of Cambridge, Cambridge, U.K., in 2005 and 2007, respectively, and the Ph.D. degree in engineering for research on radio over fiber systems and distributed antenna systems from the University of Cambridge in 2009.

Currently, he is working as a Postdoctoral Research Associate with the University of Cambridge, working on optical fiber and distributed antenna systems and RFID. He has authored and coauthored over 30 peer reviewed journal and conference papers.

Dr. Crisp is a Fellow of the ERA Foundation and and Co-Founder of PervaID. He was the recipient of The Royal Academy of Engineering ERA Foundation Entrepreneurs Award in 2011.

Richard V. Penty (M'00–SM'08) received the Ph.D. degree in engineering for his research on optical fiber devices for signal processing applications from the University of Cambridge, Cambridge, U.K., in 1989.

Currently, he is a Professor of Photonics with the University of Cambridge, as well as Master of Sidney Sussex College, having previously held academic posts at the Universities of Bath and Bristol. He has authored more than 750 refereed journal and conference papers. He is a Co-Founder of Zinwave Ltd. and PervasID Ltd. His research interests include high-speed optical communications systems, photonic integration, optical switching, and RFID-based sensing systems.

Prof. Penty is a Fellow of the Royal Academy of Engineering and the IET. He is an Editor-in-Chief of the *IET Optoelectronics Journal*.

Ian H. White (S'82–M'83–SM'00–F'04) received the B.A. and Ph.D. degrees in electrical sciences from the University of Cambridge, Cambridge, U.K., in 1980 and 1984, respectively.

He was appointed as Research Fellow and Assistant Lecturer with the University of Cambridge before he became a Professor of physics with the University of Bath, Bath, U.K., in 1990. In 1996, he moved to the University of Bristol, Bristol, U.K., where he was a Professor of Optical Communications, Head of the Department of Electrical and Electronic Engineering, in 1998, and Deputy Director of the Centre for Communications Research. He returned to the University of Cambridge in October 2001 as van Eck Professor of Engineering. Currently, he is a Master of Jesus College, Cambridge, Deputy Vice Chancellor of the University, and Head of the Photonic Research Group, with the Engineering Department, University of Cambridge. He is involved in policy development and administration of research and a number of international conference committees. He is a Co-Founder of Zinwave Ltd. He has authored more than 900 journal and conference papers, and 20 patents.

Prof. White is a Fellow of the Royal Academy of Engineering.

Qi Zhang (S'10) received the B.A. degree in electric and information science from the University of Cambridge, Cambridge, U.K., in 2010, and the M.A. and M.Eng. degrees in electrical engineering from the University of Cambridge, Cambridge, U.K., in 2011. Currently, he is pursuing the Ph.D. degree in electrical and information science at the Centre for Photonic Systems Group, University of Cambridge.

His research interests include distributed antenna networks, and RFID sensing and location.